Chapter 9

Neutrino and Electron Scattering from Point Particles

9.1 Introduction

We have seen in Chapter 8, that the standard model for the leptons developed by Salam [37] and Weinberg [157], which was later extended to the quark sector by Glashow [64], unifies weak and electromagnetic interactions. It predicts, in a unique way, the interaction Lagrangian for charge changing (CC) weak interactions of leptons and neutrinos of all flavors with charged gauge vector bosons, $W^{\pm}$ and the electromagnetic interactions of charged leptons with photons. It also predicts the existence of neutral current(NC) weak interactions of charged leptons and neutrinos of all flavors with the neutral gauge boson, Z^0. The strength of the interaction of the charged, neutral, and electromagnetic currents with the $W^{\pm}$, Z^0, and A gauge bosons are described in terms of the weak coupling constants g, electromagnetic coupling constant e, and a free parameter θ_W called the weak mixing angle. Specifically, the interaction Lagrangian discussed in Chapter 8 is written here again as:

$$L_I = -e\left[\frac{1}{2\sqrt{2}\sin\theta_W}\left(j_\mu^{\rm CC}W^{\mu+} + \text{h.c.}\right) + \frac{1}{2\sin\theta_W\cos\theta_W}j_\mu^{\rm NC}Z^\mu + j_\mu^{\rm EM}A^\mu\right], \quad (9.1)$$

where $W_\mu^{\pm}$, Z_μ, and A_μ are the charged, neutral and electromagnetic gauge fields and

$$j_\mu^{\rm CC} = \sum_{l=e,\mu,\tau}\overline{\psi}_l\gamma_\mu(1-\gamma^5)\psi_{\nu_l}, \quad (9.2)$$

$$j_\mu^{\rm NC} = \sum_{l=e,\mu,\tau}\left[\overline{\psi}_l\gamma_\mu(g_V^l - g_A^l\gamma^5)\psi_l + \overline{\psi}_{\nu_l}\gamma_\mu(g_V^{\nu_l} - g_A^{\nu_l}\gamma^5)\psi_{\nu_l}\right], \quad (9.3)$$

$$j_\mu^{\rm EM} = \sum_{l=e,\mu,\tau}\overline{\psi}_l\gamma_\mu\psi_l, \quad (9.4)$$

https://doi.org/10.1017/9781108489065.010 Published online by Cambridge University Press

with $\sin\theta_W = \frac{e}{g}$, $g_V^l = -\frac{1}{2} + 2\sin^2\theta_W$, $g_A^l = -\frac{1}{2}$, $g_V^{\nu_l} = \frac{1}{2}$ and $g_A^{\nu_l} = \frac{1}{2}$, where $e = \sqrt{4\pi\alpha}$, α is the fine structure constant. In the following sections, we use the interaction Lagrangian in Eq. (9.1) to calculate the cross sections for some weak and electromagnetic processes using point particles, that is, charged leptons and neutrinos.

9.2 $e^- + \mu^- \longrightarrow e^- + \mu^-$ scattering

This scattering process can take place through an electromagnetic process mediated by a virtual photon as well as by the weak neutral current mediated by a Z^0 boson in the standard model [400].

When an electron interacts with a photon field (Figure 9.1(a)), the interaction Lagrangian is given by:

$$\mathcal{L}_I^{\text{em}} = -e\overline{\psi}_e(\vec{k}')\gamma^\mu\psi_e(\vec{k})A_\mu \tag{9.5}$$

and when it interacts with the Z^0 boson field (Figure 9.2(a)), the Lagrangian is given by:

$$\mathcal{L}_I^{\text{NC}} = \frac{-g}{2\cos\theta_W}\bar{\psi}(\vec{k}')\gamma_\mu(g_V^e - g_A^e\gamma^5)\psi(\vec{k})Z^\mu. \tag{9.6}$$

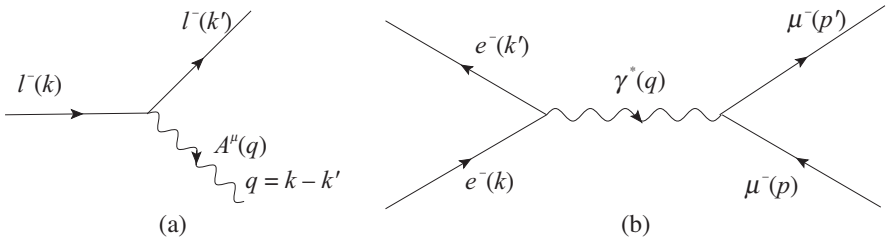

Figure 9.1 (a) Left panel: Interaction of a charged lepton with a photon field. (b) Right panel: Feynman diagram for $e^- - \mu^-$ scattering. The quantities in the brackets are the respective four momenta of the particles and q is the four momentum transfer.

Using the aforementioned Lagrangians corresponding to Figure 9.1(b) and following the Feynman rules the transition amplitude $\mathcal{M}$ for the process

$$e^-(\vec{k}, E_e) + \mu^-(\vec{p}, E_\mu) \longrightarrow e^-(\vec{k}', E_e') + \mu^-(\vec{p}\,', E_\mu') \tag{9.7}$$

mediated through virtual photon exchange of momentum $q = k - k'$, in the lowest order, may be written as:

$$-i\mathcal{M}_\gamma \;=\; \bar{u}(\vec{k}')ie\gamma^\mu u(\vec{k})\left(\frac{-ig_{\mu\nu}}{q^2}\right)\bar{u}(\vec{p}')ie\gamma^\nu u(\vec{p}) \tag{9.8}$$

and for the process mediated through the virtual Z^0 exchange, shown by the Feynman diagram in Figure 9.2(b) as:

$$-i\mathcal{M}_{Z^0} \;=\; \left[\bar{u}(\vec{k}')\left(\frac{-ig}{2\cos\theta_W}\right)\gamma_\mu(g_V^e - g_A^e\gamma_5)u(\vec{k})\right]\left(\frac{-ig^{\mu\nu}}{M_Z^2}\right)\left[\bar{u}(\vec{p}')\left(\frac{-ig}{2\,\cos\theta_W}\right)\right.$$

https://doi.org/10.1017/9781108489065.010 Published online by Cambridge University Press

$$\times\ \gamma_\nu(g_V^\mu - g_A^\mu\gamma_5)u(\vec{p})\Big],$$

$$\Rightarrow \mathcal{M}_{Z^0} = \left(\frac{-g^2}{4M_Z^2\cos^2\theta_W}\right)\left[\bar{u}(\vec{k}')\gamma_\mu(g_V^e - g_A^e\gamma_5)u(\vec{k})\right]\left[\bar{u}(\vec{p}')\gamma^\mu(g_V^\mu - g_A^\mu\gamma_5)u(\vec{p})\right], \tag{9.9}$$

where $g_V^e = g_V^\mu = -\frac{1}{2} + 2\sin^2\theta_W$ and $g_A^e = g_A^\mu = -\frac{1}{2}$. The process proceeding through Z^0 is highly suppressed as compared to the photon exchange ($\sigma_\gamma \approx 10^5 \times \sigma_{Z^0}$), therefore, in the present case, we present the cross section for the process given in Eq. (9.7) mediating through γ-exchange.

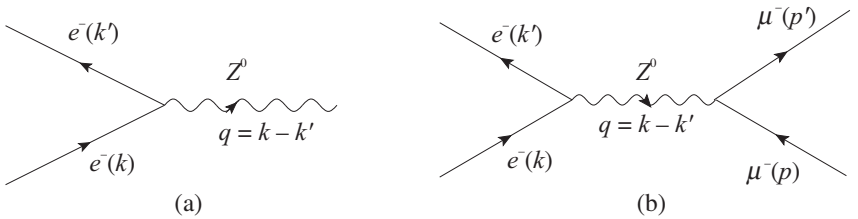

Figure 9.2 (a) Left panel: Lepton interacting with the Z^0 field. (b) Right panel: Feynman diagram for $e^- - \mu^-$ scattering via Z^0 field interaction. The quantities in the brackets are the respective four momenta of the particles and q is the four momentum transfer.

Current conservation holds good at each of the vertices, that is, $\partial^\mu J_\mu = 0$, which may be verified in the momentum space as:

$$\bar{u}(\vec{p}')q^\mu\gamma_\mu u(\vec{p}) = \bar{u}(\vec{p}')\not{q}u(\vec{p}) = \bar{u}(\vec{p}')(\not{p}' - \not{p})u(\vec{p}) = 0,$$

where the Dirac equation (in the momentum space) has been used, that is, $(\not{p} - m)\,u(\vec{p}) = 0$. In the case of unpolarized e^- and μ^-, we average over the initial spins and sum over the final spins. Using the standard projection operators for spin $\frac{1}{2}$ spinors (Appendix D), we may write:

$$\begin{aligned}\overline{\sum}\sum|\,\mathcal{M}_\gamma\,|^2 &= \frac{1}{2}\cdot\frac{1}{2}\cdot\frac{e^4}{q^4}\cdot Tr\left[(\not{k}' + m_e)\right.\\ &\qquad \left.\gamma^\mu(\not{k} + m_e)\gamma^\nu\right]\cdot Tr\left[(\not{p}' + m_\mu)\gamma_\mu(\not{p} + m_\mu)\gamma_\nu\right]\\ &= \frac{e^4}{4q^4}L_e^{\mu\nu}L_{\mu\nu}^{\text{muon}},\end{aligned} \tag{9.10}$$

where the symbol $\overline{\sum}$ represents the average taken over initial spins which gives a factor of $\frac{1}{2}$ each for e^- and μ^- and $\sum$ represents the sum over the final spin states. m_e and m_μ are the masses of electron and muon, respectively. The electronic tensor $L_e^{\mu\nu}$ and the muonic tensor $L_{\mu\nu}^{\text{muon}}$ are given as (Appendix D):

$$L_e^{\mu\nu} = Tr\left[(\not{k}' + m_e)\gamma^\mu(\not{k} + m_e)\gamma^\nu\right] = 4[k^\mu k'^\nu + k'^\mu k^\nu - (k\cdot k' - m_e^2)g^{\mu\nu}], \tag{9.11}$$

$$L_{\mu\nu}^{\text{muon}} = Tr\left[(\not{p}' + m_\mu)\gamma_\mu(\not{p} + m_\mu)\gamma_\nu\right] = 4[p_\mu p'_\nu + p'_\mu p_\nu - (p\cdot p' - m_\mu^2)g_{\mu\nu}]. \tag{9.12}$$

https://doi.org/10.1017/9781108489065.010 Published online by Cambridge University Press

Contraction of $L_e^{\mu\nu}$ and $L_{\mu\nu}^{\text{muon}}$ gives us the following expression for the matrix element squared, when averaged over the initial spin states and summed over the final spin states leading to

$$\Rightarrow \quad \overline{\sum}\sum \mid \mathcal{M}_\gamma \mid^2 \;=\; \frac{4e^4}{q^4}\Big\{2(k\cdot p)(k'\cdot p') + 2(k\cdot p')(k'\cdot p) - 2(p\cdot p' - m_\mu^2)(k\cdot k') \\ -2(k\cdot k' - m_e^2)(p\cdot p') + 4(k\cdot k' - m_e^2)(p\cdot p' - m_\mu^2)\Big\}. \quad (9.13)$$

Defining the four momentum transfer $q = k - k' = p' - p$, and $q^2 = -2k.k' = -2EE'(1 - \cos\theta)$, in the limit of $m_e \to 0$, the expression reduces to

$$\overline{\sum}\sum \mid \mathcal{M}_\gamma \mid^2 = \left[\frac{8e^4}{q^4}\Big\{2k'\cdot p\, k\cdot p + (-q^2/2)k\cdot p + (q^2/2)k'\cdot p - m_\mu^2 k\cdot k'\Big\}\right].$$

In the Lab frame, the target particle is at rest(Figure 9.3), that is, $\vec{p} = 0$, $E_\mu = m_\mu$, which leads to $k\cdot p = m_\mu E_e$ and $k'\cdot p = m_\mu E'_e$.

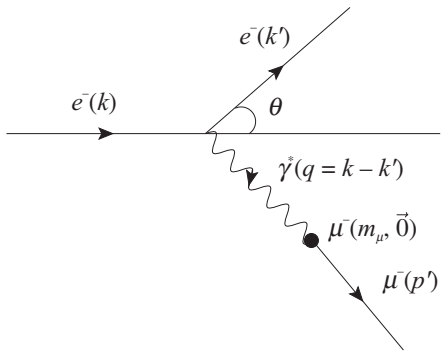

Figure 9.3 $e^- - \mu^-$ scattering in the laboratory frame. q is the four momentum transfer, that is, $q = k - k' = p' - p$. θ is the Lab scattering angle.

In this frame, $\overline{\sum}\sum \mid \mathcal{M}_\gamma \mid^2$ is derived to be (Appendix D):

$$\overline{\sum}\sum \mid \mathcal{M}_\gamma \mid^2 \;=\; \left[\frac{8e^4}{q^4}\left\{2m_\mu^2 E_e E'_e - \frac{q^2}{2}m_\mu(E_e - E'_e) + \frac{m_\mu^2 q^2}{2}\right\}\right] \\ =\; \left\{\frac{8e^4}{q^4}2m_\mu^2 E_e E'_e\left[\cos^2\frac{\theta}{2} - \frac{q^2}{2m_\mu^2}\sin^2\frac{\theta}{2}\right]\right\}. \quad (9.14)$$

If the outgoing electron is to be observed, then the integration over momenta of the outgoing muon is to be performed and vice versa.

In the Lab frame, the differential scattering cross section is given by (Appendix E):

$$\left.\frac{d\sigma}{d\Omega_e}\right|_{\text{Lab}} \;=\; \frac{1}{64\pi^2 m_\mu E_e}\overline{\sum}\sum|\mathcal{M}_\gamma|^2\frac{|\vec{k}'|^3}{((E_e + m_\mu)|\vec{k}'|^2 - \vec{k}\cdot\vec{k}'E'_e)} \quad (9.15)$$

https://doi.org/10.1017/9781108489065.010 Published online by Cambridge University Press

which leads to

$$\left.\frac{d\sigma}{d\Omega_e}\right|_{\text{Lab}} = \frac{\alpha^2}{4E_e^2 \sin^4(\frac{\theta}{2})} \frac{E_e'}{E_e} \left\{ \cos^2\frac{\theta}{2} - \frac{q^2}{2m_\mu^2} \sin^2\frac{\theta}{2} \right\} \tag{9.16}$$

and the total scattering cross section σ is given by:

$$\sigma|_{\text{Lab}} = 2\pi \int_{-1}^{+1} d(\cos\theta) \frac{\alpha^2}{4E_e^2 \sin^4(\frac{\theta}{2})} \frac{E_e'}{E_e} \left\{ \cos^2\frac{\theta}{2} - \frac{q^2}{2m_\mu^2} \sin^2\frac{\theta}{2} \right\}. \tag{9.17}$$

Figure 9.4 presents the results for $\left.\frac{d\sigma}{d\Omega}\right|_{\text{Lab}}$ vs. $\cos\theta$ at various values of incident electron energies, viz., $E_e = 20$, 50, 100, 200 and 500 MeV. It may be observed that the differential scattering cross section is forward peaked. When the expression given in Eq. (9.16) is compared

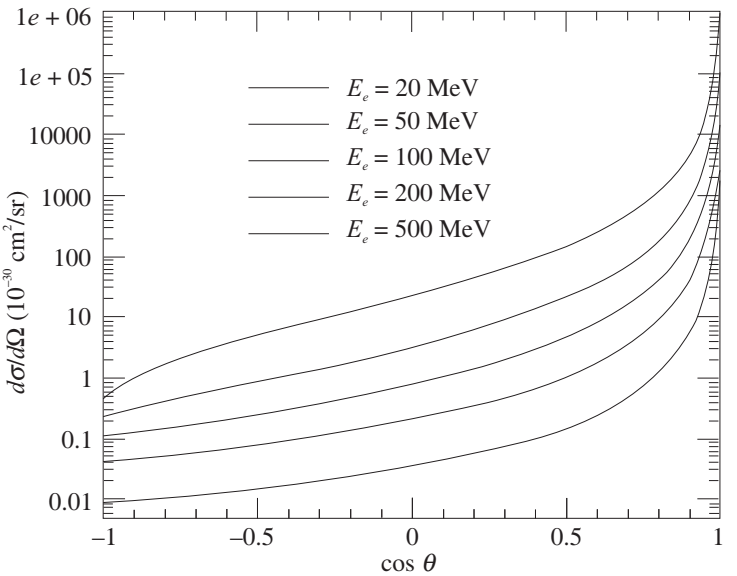

Figure 9.4 $\frac{d\sigma}{d\Omega}$ vs. $\cos\theta$ at various values of incident electron energies viz. $E_e = 20$, 50, 100, 200 and 500 MeV evaluated in the Lab frame.

with the results of $d\sigma/d\Omega$ for the scattering of e^- with a spinless ($J = 0$) point target (i.e., without any structure) known as Mott scattering cross section, which will be discussed in Chapter 10, one obtains:

$$\left.\frac{d\sigma}{d\Omega}\right|_{\text{spinless}} = \frac{\alpha^2}{4E_e^2 \sin^4\theta/2} . \frac{E_e'}{E_e} \cos^2\frac{\theta}{2}$$

$$\Rightarrow \quad \frac{\left.\frac{d\sigma}{d\Omega}\right|_{e^-\mu^- \to e^-\mu^-}}{\left.\frac{d\sigma}{d\Omega}\right|_{\text{spinless}}} = 1 + \frac{Q^2}{2m_\mu^2} \tan^2\frac{\theta}{2}, \tag{9.18}$$

https://doi.org/10.1017/9781108489065.010 Published online by Cambridge University Press

where $Q^2 = -q^2 \geq 0$. The extra factor in Eq. (9.18) (i.e., $\frac{Q^2}{2m_\mu^2}\sin^2\frac{\theta}{2}$) is due to the presence of the spin content of the muon and is considered to be the contribution of the muon magnetic moment to the scattering cross section. One may also express the cross section in the center of

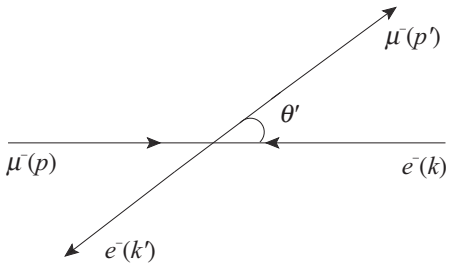

Figure 9.5 $e^- - \mu^-$ scattering in the center of mass (CM) frame. θ' is the CM scattering angle.

mass (CM) frame (Figure 9.5), in which

$$\begin{aligned} k\cdot p &= k'\cdot p' = \frac{s-m_e^2-m_\mu^2}{2}; \qquad & k\cdot k' &= -\frac{t-2m_e^2}{2}; \\ k\cdot p' &= k'\cdot p = -\frac{u-m_e^2-m_\mu^2}{2}; \qquad & p\cdot p' &= -\frac{t-2m_\mu^2}{2}, \end{aligned} \tag{9.19}$$

where s, t, u are the Mandelstam variables defined as:

$$s = (k+p)^2 = (k'+p')^2;\ \ t = (k-k')^2 = (p'-p)^2 \ \text{ and } \ u = (k-p')^2 = (k'-p)^2. \tag{9.20}$$

The general expression for the differential scattering cross section in CM frame is given as (Appendix E):

$$\left.\frac{d\sigma}{d\Omega}\right|_{CM} = \frac{1}{64\pi^2 s}\overline{\sum}\sum|\mathcal{M}_\gamma|^2. \tag{9.21}$$

Using the values of s, t, and u from Eq. (9.20) in Eq. (9.21), the differential cross section in the CM frame becomes,

$$\begin{aligned} \left.\frac{d\sigma}{d\Omega}\right|_{CM} &= \frac{1}{16\pi^2 s}\frac{e^4}{t^2}\left[\frac{(s-m_e^2-m_\mu^2)^2}{2}+\frac{(u-m_e^2-m_\mu^2)^2}{2}-\left(\frac{t}{2}\right)(t-2m_e^2)\right. \\ &- \left.\left(\frac{t}{2}\right)(t-2m_\mu^2)+t^2\right]. \end{aligned} \tag{9.22}$$

In the relativistic limit, that is, $E_e >> m_e$ and $E_\mu >> m_\mu$, we get

$$\left.\frac{d\sigma}{d\Omega}\right|_{CM} = \frac{1}{32\pi^2 s}e^4\left(\frac{s^2+u^2}{t^2}\right). \tag{9.23}$$

https://doi.org/10.1017/9781108489065.010 Published online by Cambridge University Press

9.3 $\nu_\mu + e^- \to \mu^- + \nu_e$ scattering

This process is also known as inverse muon decay and is expressed as:

$$\nu_\mu(\vec{k}, E_{\nu_\mu}) + e^-(\vec{p}, E_e) \longrightarrow \mu^-(\vec{k}', E_\mu) + \nu_e(\vec{p}\,', E_{\nu_e}). \tag{9.24}$$

The scattering is a charge changing process at (ν_μ, μ^-) and (e^-, ν_e) vertices. In this process, a ν_μ of momentum k gets converted into a μ^- of momentum k' by emitting a virtual W^+ boson which is absorbed by the electron of momentum p and gets converted into a ν_e of momentum p'.

The interaction Lagrangian for the leptons interacting with a W^+ field is given by:

$$\mathcal{L}_I = \frac{-g}{2\sqrt{2}}\bar{\psi}(\vec{k}')\gamma_\mu(1-\gamma_5)\psi(\vec{k})W^{+\mu}. \tag{9.25}$$

Using this Lagrangian, we obtain the transition amplitude using Feynman rules, in the limit of $q^2 << M_W^2$, for the Feynman diagram depicted in Figure 9.6 as:

$$-i\mathcal{M}_{\rm CC} = \bar{u}(\vec{k}')\left[\frac{-ig}{2\sqrt{2}}\gamma^\mu(1-\gamma_5)\right]u(\vec{k})\left(\frac{-ig_{\mu\nu}}{M_W^2}\right)\bar{u}(\vec{p}\,')\left[\frac{-ig}{2\sqrt{2}}\gamma^\nu(1-\gamma_5)\right]u(\vec{p})$$

$$\implies \quad \mathcal{M}_{\rm CC} = \frac{-g^2}{8M_W^2}[\bar{u}(\vec{k}')\gamma^\mu(1-\gamma_5)u(\vec{k})][\bar{u}(\vec{p}\,')\gamma_\mu(1-\gamma_5)u(\vec{p})] \tag{9.26}$$

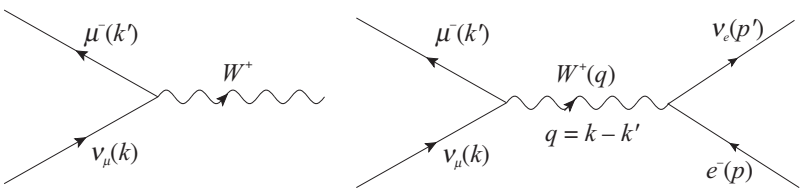

Figure 9.6 (a) Left panel: ν_μ interaction with a W field. (b) Right panel: Charged current interaction $\nu_\mu e^- \to \mu^-\nu_e$.

and

$$\overline{\sum_i}\sum_f |\mathcal{M}|^2 = \frac{1}{2}\frac{G_F^2}{2}L^{\mu\nu}_{\rm muon}L^{\rm electron}_{\mu\nu},$$

where $\overline{\sum}_i$ represents the average taken over the spin of initial particles which gives a factor of $\frac{1}{2}$ due to the electron, as ν_μ has only one component being left handed. In this expression,

$$L^{\mu\nu}_{\rm muon} = \sum_{\mu,\nu=0}^{3} Tr\left[(\not{k}' + m_\mu)\gamma^\mu(1-\gamma_5)(\not{k})\gamma^\nu(1-\gamma_5)\right], \tag{9.27}$$

which leads to (Appendix D):

$$L^{\mu\nu}_{\rm muon} = 8\left[k^\mu k'^\nu + k'^\mu k^\nu - g^{\mu\nu}k\cdot k' + i\epsilon^{\mu\nu\alpha\beta}k_\alpha k'_\beta\right] \tag{9.28}$$

https://doi.org/10.1017/9781108489065.010 Published online by Cambridge University Press

and

$$L_{\mu\nu}^{\text{electron}} = \sum_{\mu,\nu=0}^{3} Tr\left[\not{p}'\gamma_\mu(1-\gamma_5)(\not{p}+m_e)\gamma_\nu(1-\gamma_5)\right], \tag{9.29}$$

which leads to (Appendix D):

$$L_{\mu\nu}^{\text{electron}} = 8\left[p_\mu p'_\nu + p'_\mu p_\nu - g_{\mu\nu}p\cdot p' - i\epsilon_{\mu\nu\sigma\rho}p^\sigma p'^\rho\right]. \tag{9.30}$$

Contraction of $L_{\text{muon}}^{\mu\nu}$ with $L_{\mu\nu}^{\text{electron}}$ is similar to what has been discussed in the case of $e^-\mu^-$ scattering, but besides the symmetric terms, there will be an additional term from the antisymmetric part because of the following property of the tensors

$$\epsilon_{\mu\nu\alpha\beta}\epsilon^{\mu\nu\sigma\rho} = 2(\delta_\alpha^\sigma\delta_\beta^\rho - \delta_\alpha^\rho\delta_\beta^\sigma). \tag{9.31}$$

Incorporating this property, the matrix element squared becomes

$$\overline{\sum_i}\sum_f |\mathcal{M}|^2 = 64G_F^2(k\cdot p)(k'\cdot p'). \tag{9.32}$$

In the Lab frame for the initial electron at rest, we have

$$k\cdot p \;=\; m_e E_{\nu_\mu};\;\; k\cdot k' = E_{\nu_\mu}E_\mu - E_{\nu_\mu}|\vec{k}'|\cos\theta \;\text{ and }\; k'\cdot p' = k'\cdot(k-k'+p),$$

which results in

$$\overline{\sum_i}\sum_f |\mathcal{M}|^2 = 64G_F^2(m_e E_{\nu_\mu})\left[E_{\nu_\mu}E_\mu - E_{\nu_\mu}|\vec{k}'|\cos\theta + m_e E_\mu - m_\mu^2\right]. \tag{9.33}$$

The expression for the differential cross section in the Lab frame is then given by:

$$\left.\frac{d\sigma}{d\Omega}\right|_{\text{Lab}} \;=\; \frac{1}{\pi^2 m_e}G_F^2\frac{E_\mu^2}{E_{\nu_\mu}}\left[E_{\nu_\mu}E_\mu - E_{\nu_\mu}|\vec{k}'|\cos\theta + m_e E_\mu - m_\mu^2\right] \tag{9.34}$$

and the total scattering cross section σ, in the relativistic limit, that is, $|\vec{p}\,| = E$, is given by:

$$\sigma = 2\pi\int_{-1}^{+1} d(cos\theta)\frac{1}{\pi^2 m_e}G_F^2\frac{E_\mu^2}{E_{\nu_\mu}}\left[E_{\nu_\mu}E_\mu - E_{\nu_\mu}|\vec{k}'|\cos\theta + m_e E_\mu - m_\mu^2\right]. \tag{9.35}$$

The expression for the differential cross section in the CM frame is given as:

$$\left.\frac{d\sigma}{d\Omega}\right|_{CM} = \frac{G_F^2}{4\pi^2 s}\left[(s-m_e^2)(s-m_\mu^2)\right], \tag{9.36}$$

where $s = (k+p)^2 = E_{CM}^2$.

In 1980, the CHARM collaboration studied the inverse muon decay using wide band neutrino and antineutrino beams from CERN SPS; a total number of 171 ± 29 events for $\nu_\mu + e^- \rightarrow \mu^- + \nu_e$ were observed [265]. The observed rates were in agreement with the prediction derived for $V-A$ theory and for left-handed two-component neutrinos. Later, in 1990, CHARM-II

https://doi.org/10.1017/9781108489065.010 Published online by Cambridge University Press

collaboration performed the $\nu_\mu + e^- \rightarrow \mu^- + \nu_e$ scattering experiment and found the value of the cross section to be $(18.16 \pm 1.36) \times 10^{-42}\text{cm}^2\text{GeV}^{-1}$ [401]. A similar experiment was performed at the Tevatron, Fermilab, where the cross section was measured and found to be $\sigma(\nu_\mu e^- \longrightarrow \mu^- \nu_e) = [16.93 \pm 0.85(stat.) \pm 0.52(syst.)] \times E \times 10^{-42}$ cm^2 [266], which is consistent with the theoretically predicted value obtained using the standard model.

9.4 $\nu_\mu + e^- \rightarrow \nu_\mu + e^-$ scattering

The process

$$\nu_\mu(\vec{k}, E_{\nu_\mu}) + e^-(\vec{p}, E_e) \rightarrow \nu_\mu(\vec{k}', E'_{\nu_\mu}) + e^-(\vec{p}\,', E'_e) \tag{9.37}$$

is a neutral current induced process, mediated by a Z^0 boson, in the standard model. In this process, a ν_μ of momentum k emits a Z^0 boson that gets absorbed by an electron of momentum p.

The interaction Lagrangian for $\nu\nu Z$ interaction, shown in Figure 9.7(a), is given as:

$$\mathcal{L}_I^{\text{neutrino}} = \frac{-g}{2\cos\theta_W}\bar{\psi}(\vec{k}')\gamma_\mu(g_V^\nu - g_A^\nu\gamma^5)\psi(\vec{k})Z^\mu. \tag{9.38}$$

Similarly, the interaction Lagrangian at the electron vertex shown in Figure 9.7(b) is given by:

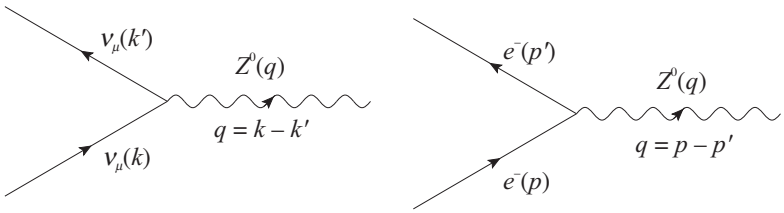

Figure 9.7 (a) Left panel: Neutrino interacting with the Z^0 field. (b) Right panel: Electron interacting with the Z^0 field.

$$\mathcal{L}_I^{\text{electron}} = \frac{-g}{2cos\theta_W}\bar{\psi}(\vec{p}\,')\gamma_\mu(g_V^e - g_A^e\gamma^5)\psi(\vec{p})Z^\mu. \tag{9.39}$$

Using the interaction Lagrangians given in Eqs. (9.38) and (9.39), the transition matrix element, corresponding to the Feynman diagram shown in Figure 9.8 is given by:

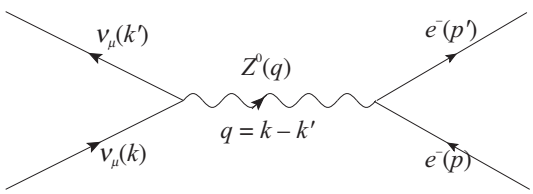

Figure 9.8 Neutral current reaction for the process $\nu_\mu + e^- \longrightarrow \nu_\mu + e^-$.

https://doi.org/10.1017/9781108489065.010 Published online by Cambridge University Press

$$-i\mathcal{M}_{\rm NC} = \left[\bar{u}(\vec{k}')\left(\frac{-ig}{2\,cos\theta_W}\right)\gamma_\mu(g_V^\nu - g_A^\nu\gamma_5)u(\vec{k})\right]\left(\frac{-ig^{\mu\nu}}{M_Z^2}\right)\left[\bar{u}(\vec{p}')\left(\frac{-ig}{2\,cos\theta_W}\right)\right.$$
$$\left.\times\ \gamma_\nu(g_V^e - g_A^e\gamma_5)u(\vec{p})\right],$$

with $g_V^\nu = \frac{1}{2}, g_A^\nu = \frac{1}{2}$, $g_V^e = -\frac{1}{2} + 2\sin^2\theta_W$, and $g_A^e = -\frac{1}{2}$. The expression for square of the invariant matrix element for the reaction given in Eq. (9.37) is obtained as:

$$\overline{\sum_i}\sum_f|\mathcal{M}|^2 = \frac{1}{2}\left(\frac{4G_F^2}{2}\right)L_{\mu\nu}^{\rm neutrino}L_{\rm electron}^{\mu\nu}$$

where $\frac{1}{2}$ is due to the averaging over the initial electron spin, $\frac{G_F}{\sqrt{2}} = \frac{g^2}{8M_Z^2\cos^2\theta_W}$ and the leptonic tensors are obtained as:

$$L_{\mu\nu}^{\rm neutrino} = 2\left[k_\mu k'_\nu + k'_\mu k_\nu - g_{\mu\nu}k\cdot k' - i\epsilon_{\sigma\mu\rho\nu}k^\rho k'^\sigma\right],$$

$$L_{\rm electron}^{\mu\nu} = 4\left[\{(g_V^e)^2 + (g_A^e)^2\}(p'^\mu p^\nu - p'\cdot p g_{\mu\nu} + p'^\nu p^\mu) + 2p'_\lambda p_\theta i\epsilon^{\lambda\mu\theta\nu}g_V^e g_A^e\right.$$
$$\left.+m_e^2 g^{\mu\nu}\{(g_V^e)^2 - (g_A^e)^2\}\right].$$

The contraction of the leptonic tensors ($L_{\mu\nu}^{\rm neutrino}$ and $L_{\rm electron}^{\mu\nu}$), gives:

$$\overline{\sum_i}\sum_f|\mathcal{M}|^2 = 16\,G_F^2\left[(g_V^e + g_A^e)^2(k'\cdot p')(k\cdot p) + (g_V^e - g_A^e)^2(k'\cdot p)(k\cdot p')\right.$$
$$\left.-\ m_e^2\{(g_V^e)^2 - (g_A^e)^2\}(k\cdot k')\right].$$

In the Lab frame, the initial electron is at rest and we have

$$k\cdot p = m_e E_\nu,\ k\cdot p' = E_\nu E'_e - E_\nu|\vec{p}'|\cos\theta,\quad \theta \text{ is the Lab scattering angle}$$
$$k\cdot k' = E_\nu m_e - E_\nu E'_e\ +\ E_\nu|\vec{p}'|\cos\theta,\ k'\cdot p' = E_\nu E'_e - E_\nu|\vec{p}'|\cos\theta + m_e E'_e - m_e^2$$
$$\text{and } k'\cdot p = (k + p - p')\cdot p = m_e E_\nu + m_e^2 - m_e E'_e. \tag{9.40}$$

Therefore,

$$\overline{\sum_i}\sum_f|\mathcal{M}|^2 = 16\,G_F^2 m_e E_\nu\left[(g_V^e + g_A^e)^2(E_\nu E'_e - E_\nu|\vec{p}'|\cos\theta + m_e E'_e - m_e^2)\right.$$
$$+\ (g_V^e - g_A^e)^2(E_\nu + m_e - E'_e)(E'_e - |\vec{p}'|\cos\theta)$$
$$\left.-\ m_e\{(g_V^e)^2 - (g_A^e)^2\}(m_e - E'_e + |\vec{p}'|\cos\theta)\right], \tag{9.41}$$

https://doi.org/10.1017/9781108489065.010 Published online by Cambridge University Press

and the expression for the differential cross section in the Lab frame is obtained as:

$$\left.\frac{d\sigma}{d\Omega}\right|_{\rm Lab} = \frac{1}{4\pi^2 m_e} G_F^2 \left(\frac{E_e'^2}{E_\nu}\right) \Big[(g_V^e + g_A^e)^2 (E_\nu E_e' - E_\nu |\vec{p}\,'| \cos\theta + m_e E_e' - m_e^2) + (g_V^e - g_A^e)^2 (E_\nu + m_e - E_e')(E_e' - |\vec{p}\,'| \cos\theta) - m_e \{(g_V^e)^2 - (g_A^e)^2\}(m_e - E_e' + |\vec{p}\,'| \cos\theta)\Big]. \quad (9.42)$$

The total scattering cross section is then given as:

$$\sigma = 2\pi \int_{-1}^{+1} d(cos\theta) \frac{1}{4\pi^2 m_e} G_F^2 \left(\frac{E_e'^2}{E_\nu}\right) \Big[(g_V^e + g_A^e)^2 (E_\nu E_e' - E_\nu |\vec{p}\,'| \cos\theta + m_e E_e' - m_e^2) + (g_V^e - g_A^e)^2 (E_\nu + m_e - E_e')(E_e' - |\vec{p}\,'| \cos\theta) - m_e \{(g_V^e)^2 - (g_A^e)^2\} (m_e - E_e' + |\vec{p}\,'| \cos\theta)\Big].$$

The expression for the differential cross section in CM frame is obtained as:

$$\left.\frac{d\sigma}{d\Omega}\right|_{CM} = \frac{1}{4\pi^2 s} G_F^2 \Big[(g_V^e + g_A^e)^2 \Big(\frac{s - m_e^2}{2}\Big)^2 + (g_V^e - g_A^e)^2 \Big(\frac{u - m_e^2}{2}\Big)^2 + \frac{m_e^2}{2} \{(g_V^e)^2 - (g_A^e)^2\} t\Big], \quad (9.43)$$

where $s = (k + p)^2 = E_{CM}^2$. A similar expression may be obtained for $\bar{\nu}_\mu + e^- \to \bar{\nu}_\mu + e^-$ differential scattering cross section, using the matrix element squared, given in Eq. (9.50) and Table 9.1.

In 1973, at CERN, the Gargamelle bubble chamber experiment [402] was used to observe for the first time $\nu_\mu e^-$ and $\bar{\nu}_\mu e^-$ events; cross section measurements were performed in the energy region of ≈ 1 GeV. The experiment also measured the weak $\sin^2\theta_W$ and put some limit on it. The CHARM collaboration [351] in 1977, performed the $\nu_\mu e^-$ cross section measurements using the CERN narrow band beam (NBB) as well as the wide band neutrino beam (WBB). In total, 83 ± 16 $\nu_\mu e^-$ and 116 ± 21 $\bar{\nu}_\mu e^-$ events were reported; the cross sections were measured and have been tabulated in Table 9.2. At the Brookhaven National Laboratory (BNL), the E734 experiment [145] measured the $\nu_\mu e^-$ and $\bar{\nu}_\mu e^-$ scattering cross sections using an alternating gradient synchrotron source (AGS) with an average energy of $\nu_\mu(\bar{\nu}_\mu) \approx 1.3$ GeV. A total number of $160 \pm 17 \pm 4$ and $97 \pm 13 \pm 5$ events were reported for $\nu_\mu e^-$ and $\bar{\nu}_\mu e^-$, respectively. Moreover, CHARM-II collaboration [403] at CERN in 1987 used CERN-SPS WBB and measured the $\nu_\mu e^-$ cross section; they also performed a high precision measurement of $\sin^2\theta_W$. The results of the experiment have been tabulated in Table 9.2. $\nu_\mu e^-$ scattering cross sections were also measured at the Fermi National Accelerator Laboratory (FNAL). The experiments were performed using wide band ν_μ beam with an average energy of 20 GeV and a maximum energy of 100 GeV. The reported cross section is [166]

$$\sigma_{\rm expt}(\nu_\mu e^- \to \nu_\mu e^-) = (1.40 \pm 0.30) \times 10^{-40} E_{\nu_\mu} cm^2/GeV.$$

These results are consistent with the standard model if one takes $\sin^2\theta_W = 0.23$.

https://doi.org/10.1017/9781108489065.010 Published online by Cambridge University Press

Table 9.1 Values of α, β, and γ for $\nu_\mu e^-$, $\overline{\nu}_\mu e^-$, $\nu_e e^-$, and $\overline{\nu}_e e^-$ scattering.

Process	α	β	γ
$\nu_\mu e^- \to \nu_\mu e^-$	$(g_V^e + g_A^e)^2$	$(g_V^e - g_A^e)^2$	$(g_A^e)^2 - (g_V^e)^2$
$\overline{\nu}_\mu e^- \to \overline{\nu}_\mu e^-$	$(g_V^e - g_A^e)^2$	$(g_V^e + g_A^e)^2$	$(g_A^e)^2 - (g_V^e)^2$
$\nu_e e^- \to \nu_e e^-$	$(g'_V + g'_A)^2$	$(g'_V - g'_A)^2$	$g'^2_A - g'^2_V$
$\overline{\nu}_e e^- \to \overline{\nu}_e e^-$	$(g'_V - g'_A)^2$	$(g'_V + g'_A)^2$	$g'^2_A - g'^2_V$

9.5 $\nu_e + e^- \to \nu_e + e^-$ scattering

The process

$$\nu_e(\vec{k}, E_{\nu_e}) + e^-(\vec{p}, E_e) \to \nu_e(\vec{k}', E'_{\nu_e}) + e^-(\vec{p}\,' E'_e) \tag{9.44}$$

induced by the Z^0 boson at the $(\nu_e \nu_e)$ and the $(e^- e^-)$ vertices as well as by W^+ boson at $(\nu_e e^-)$ vertices are mediated via both the neutral and the charged current interactions in the standard model, respectively. The Lagrangian for the charged current W^+ boson exchange is given by (Figure 9.9 (a)):

$$\mathcal{L}_{\nu_e e^- W^+} = \frac{-g}{2\sqrt{2}} \bar{\psi}(\vec{p}\,') \gamma_\mu (1 - \gamma_5) \psi(\vec{k}) W^{+\mu} \tag{9.45}$$

The Lagrangians for the neutral current Z^0 exchange between the two electrons and two neutrinos is given as (Figure 9.9 (b) and (c)):

$$L^{\nu\nu Z} = \frac{-g}{2\cos\theta_W} \bar{\psi}(\vec{k}') \gamma_\mu (g_V^\nu - g_A^\nu \gamma^5) \psi(\vec{k}) Z^\mu, \tag{9.46}$$

$$L^{eeZ} = \frac{-g}{2\cos\theta_W} \bar{\psi}(\vec{p}\,') \gamma_\mu (g_V^e - g_A^e \gamma^5) \psi(\vec{p}) Z^\mu, \tag{9.47}$$

with $g_V^\nu = \frac{1}{2}, g_A^\nu = \frac{1}{2}, g_V^e = -\frac{1}{2} + 2\sin^2\theta_W$ and $g_A^e = -\frac{1}{2}$.

Therefore, the invariant matrix element for the Feynman diagram shown in Figure 9.10(a) for the charged current reaction is written as:

$$-i\mathcal{M}^{CC} = \left[\bar{u}(\vec{p}\,') \frac{-ig}{2\sqrt{2}} \gamma_\mu (1 - \gamma_5) u(\vec{k})\right] \left(-\frac{ig^{\mu\nu}}{M_W^2}\right) \left[\bar{u}(\vec{k}') \frac{-ig}{2\sqrt{2}} \gamma_\nu (1 - \gamma_5) u(\vec{p})\right],$$

$$\Rightarrow \quad \mathcal{M}^{CC} = \frac{G_F}{\sqrt{2}} \left[\bar{u}(\vec{p}\,') \gamma_\mu (1 - \gamma_5) u(\vec{k})\right] \cdot \left[\bar{u}(\vec{k}') \gamma^\mu (1 - \gamma_5) u(\vec{p})\right], \tag{9.48}$$

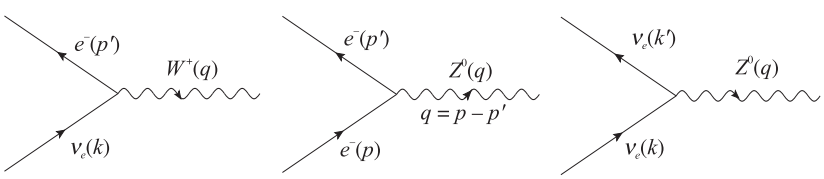

Figure 9.9 (a) Left panel: Neutrinos interacting with the W^+ field. (b) Middle panel: Electrons interacting with the Z^0 field. (c) Right panel: Neutrinos interacting with the Z^0 field.

https://doi.org/10.1017/9781108489065.010 Published online by Cambridge University Press

where

$$\frac{G_F}{\sqrt{2}} = \frac{g^2}{8M_W^2}.$$

Similarly, the matrix element for the Feynman diagram shown in Figure 9.10(b) for the neutral current reaction is given as:

$$\begin{aligned} -i\mathcal{M}_{\rm NC} &= \left[\bar{u}(\vec{k}')\frac{-ig}{2\,cos\theta_W}\gamma_\mu(g_V^\nu - g_A^\nu\gamma_5)u(\vec{k})\right] \times \left(-\frac{ig^{\mu\nu}}{M_Z^2}\right) \\ &\quad \times \left[\bar{u}(\vec{p}')\frac{-ig}{2\,cos\theta_W}\gamma_\nu(g_V^e - g_A^e\gamma_5)u(\vec{p})\right], \\ \Rightarrow\ \mathcal{M}_{\rm NC} &= \frac{G_F}{\sqrt{2}}\left[\bar{u}(\vec{k}')\gamma_\mu(1-\gamma_5)u(\vec{k})\right]\cdot\left[\bar{u}(\vec{p}')\gamma^\mu(g_V^e - g_A^e\gamma_5)u(\vec{p})\right], \end{aligned}$$

where $\frac{G_F}{\sqrt{2}} = \frac{g^2}{8M_Z^2 cos^2\theta_W}$.

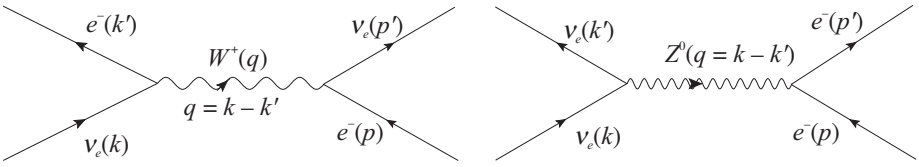

Figure 9.10 (a) Left panel: Charged current. (b) Right panel: Neutral current reactions.

Hence, the total contribution for this process from both the channels is given as:

$$\begin{aligned} \mathcal{M}_{\rm CC} + \mathcal{M}_{\rm NC} &= \frac{G_F}{\sqrt{2}}\left[\left[\bar{u}(\vec{p}')\gamma_\mu(1-\gamma_5)u(\vec{k})\right]\cdot\left[\bar{u}(\vec{k}')\gamma^\mu(1-\gamma_5)u(\vec{p})\right]\right. \\ &+ \left.\left[\bar{u}(\vec{k}')\gamma_\mu(1-\gamma_5)u(\vec{k})\right]\cdot\left[\bar{u}(\vec{p}')\gamma^\mu(g_V^e - g_A^e\gamma_5)u(\vec{p})\right]\right]. \end{aligned}$$

Making use of the Fierz transformation [258], this equation can be rewritten as:

$$\mathcal{M}_{\rm CC} + \mathcal{M}_{\rm NC} = \frac{G_F}{\sqrt{2}}\left[\bar{u}(\vec{k}')\gamma_\mu(1-\gamma_5)u(\vec{k})\right]\cdot\left[\bar{u}(\vec{p}')\gamma^\mu(g_V' - g_A'\gamma_5)u(\vec{p})\right] \quad (9.49)$$

with $g_V' = g_V^e + 1$, $g_A' = g_A^e + 1$. The expression for the matrix element square is given by:

$$\begin{aligned} \overline{\sum_i}\sum_f |\mathcal{M}|^2 &= \overline{\sum_i}\sum_f\left(|\mathcal{M}_{\rm CC}|^2 + \mathcal{M}_{\rm CC}\mathcal{M}_{\rm NC}^* + \mathcal{M}_{\rm NC}\mathcal{M}_{\rm CC}^* + |\mathcal{M}_{\rm NC}|^2\right) \\ &= 16\,G_F^2\left[(g_V' + g_A')^2(k'\cdot p')(k\cdot p) + (g_V' - g_A')^2(k'\cdot p)(k\cdot p')\right. \\ &- \left. m_e^2(g_V'^2 - g_A'^2)(k\cdot k')\right], \end{aligned}$$

where the interference term is obtained as:

$$\mathcal{M}_{\rm CC}\mathcal{M}_{\rm NC}^* + \mathcal{M}_{\rm NC}\mathcal{M}_{\rm CC}^* = 16\left[m_e^2(g_A - g_V)\,(k\cdot k') + 2(g_A + g_V)\,(k\cdot p)\,(k'\cdot p')\right].$$

https://doi.org/10.1017/9781108489065.010 Published online by Cambridge University Press

This expression may be written, in general, for other possible reactions like $\nu_\mu e^- \to \nu_\mu e^-$, $\bar{\nu}_\mu e^- \to \bar{\nu}_\mu e^-$ and $\bar{\nu}_e e^- \to \bar{\nu}_e e^-$, which may be obtained by considering both the charged and the neutral current interactions for $\nu_e e^- \to \nu_e e^-$, and only for the neutral current interactions for $\nu_\mu e^- \to \nu_\mu e^-$, $\bar{\nu}_\mu e^- \to \bar{\nu}_\mu e^-$ and $\bar{\nu}_\mu e^- \to \bar{\nu}_\mu e^-$ processes. For the antineutrino induced processes $g_A \to -g_A$, while for the ν_μ induced processes $g'_V \to g_V$, $g'_A \to g_A$, such that:

$$\overline{\sum_i}\sum_f |\mathcal{M}|^2 = 16\, G_F^2 \left[\alpha\, (k'\cdot p')(k\cdot p) + \beta\, (k'\cdot p)(k\cdot p') - \gamma\, m_e^2 (k\cdot k')\right], \qquad (9.50)$$

where the values of α, β, and γ for the various neutrino and antineutrino induced scattering off the leptons are given in Table 9.1. In the Lab frame, for the $\nu_e e^- \to \nu_e e^-$ process, the initial electron is at rest, that is, $\vec{p} = 0$. Therefore, we obtain

Table 9.2 Measured values of the total cross section and $\sin^2\theta_W$ from different experiments for $\nu_\mu e^-$ and $\bar{\nu}_\mu e^-$ scattering at 90% confidence level.

Experiment	$\sigma(\nu_\mu e^-)(\times 10^{-42}\,\frac{\text{cm}^2}{\text{GeV}})$	$\sigma(\bar{\nu}_\mu e^-)$	$\sin^2\theta_W$
Gargamelle (PS) [404]	< 1.4	$1.0\pm^{2.1}_{0.9}$	$0.1 < x < 0.4$
Aachen-Padova (PS) [167]	1.1 ± 0.6	2.2 ± 1.0	0.35 ± 0.08
Gargamelle (SPS) [404]	$2.4\pm^{1.2}_{0.9}$	< 2.7	$0.12\pm^{0.11}_{0.07}$
VMWOF(FNAL) [166]	$1.4 \pm 0.3 \pm 0.4$		$0.25 \pm^{0.07}_{0.05} \pm 0.8$
BNL-COL (AGS) [165]	1.67 ± 0.44		$0.20\pm^{0.06}_{0.05}$
BEBC-TST (SPS) [405]		< 3.4	< 0.45
15-feet. BC (FNAL) [406]		< 2.1	< 0.37
CHARM (SPS) [144]	$2.2 \pm 0.4 \pm 0.4$	$1.6 \pm 0.3 \pm 0.3$	$0.211 \pm 0.035 \pm 0.011$
BNL E734 (AGS) [145]	$1.8 \pm 0.2 \pm 0.25$	$1.17 \pm 0.16 \pm 0.13$	$0.195 \pm 0.018 \pm 0.013$
CHARM-II (SPS) [267]	$1.53 \pm 0.04 \pm 0.12$	$1.39 \pm 0.04 \pm 0.10$	$0.237 \pm 0.007 \pm 0.007$

$$\begin{aligned}\overline{\sum_i}\sum_f |\mathcal{M}|^2 \;=\; & 16\, G_F^2 m_e E_\nu \Big[(g'_V + g'_A)^2 (E_\nu E'_e - E_\nu |\vec{p}\,'| \cos\theta + m_e E'_e - m_e^2) \\ & + (g'_V - g'_A)^2 (E_\nu + m_e - E'_e)(E'_e - |\vec{p}\,'| \cos\theta) \\ & - m_e (g'^2_V - g'^2_A)(m_e - E'_e + |\vec{p}\,'| \cos\theta)\Big]. \end{aligned} \qquad (9.51)$$

The expression for the differential cross section in the Lab frame becomes

$$\begin{aligned}\left.\frac{d\sigma}{d\Omega}\right|_{\text{Lab}} \;=\; & \frac{1}{4\pi^2 m_e} G_F^2 \left(\frac{E'^2_e}{E_\nu}\right) \Big[(g'_V + g'_A)^2 (E_\nu E'_e - E_\nu |\vec{p}\,'| \cos\theta + m_e E'_e - m_e^2) \\ & + (g'_V - g'_A)^2 (E_\nu + m_e - E'_e)(E'_e - |\vec{p}\,'| \cos\theta) \\ & - m_e (g'^2_V - g'^2_A)(m_e - E'_e + |\vec{p}\,'| \cos\theta)\Big]. \end{aligned} \qquad (9.52)$$

https://doi.org/10.1017/9781108489065.010 Published online by Cambridge University Press

The total scattering cross section is given as:

$$\sigma|_{\text{Lab}} = 2\pi \int_{-1}^{+1} d(\cos\theta) \frac{1}{4\pi^2 m_e} G_F^2 \left(\frac{E_e'^2}{E_\nu}\right) \Big[(g_V' + g_A')^2 (E_\nu E_e' - E_\nu |\vec{p}\,'| \cos\theta + m_e E_e' - m_e^2) + (g_V' - g_A')^2 (E_\nu + m_e - E_e')(E_e' - |\vec{p}\,'| \cos\theta) - m_e (g_V'^2 - g_A'^2)(m_e - E_e' + |\vec{p}\,'| \cos\theta)\Big], \quad (9.53)$$

where $\vec{p}\,' = \vec{k} - \vec{k}' = \vec{q}$.

The expression for the differential cross section in the CM frame is obtained as:

$$\left.\frac{d\sigma}{d\Omega}\right|_{CM} = \frac{1}{4\pi^2 s} G_F^2 \Big[(g_V' + g_A')^2 \left(\frac{s - m_e^2}{2}\right)^2 + (g_V' - g_A')^2 \left(\frac{u - m_e^2}{2}\right)^2 + \frac{m_e^2}{2}\left\{(g_V')^2 - (g_A')^2\right\} t\Big], \quad (9.54)$$

where $s = (k + p)^2 = E_{CM}^2$.

During the late 1980s, the E225 experiment [407] was conducted at the Los Alamos Meson Physics Facility (LAMPF) to measure $\nu_e e$ scattering cross section; a total of 236±35 events were reported. The collaboration reported the measurement of an interference term arising due to the contribution of charged current (CC) and neutral current (NC) amplitudes. The value was

$$I = -1.07 \pm 0.17 \pm 0.11,$$

which was found to be in good agreement with the standard model prediction of -1.07 with $\sin^2\theta_W = 0.233$. The collaboration also reported a lower limit on the magnetic moment of the neutrino. LAMPF used neutrino beams from the muon decay at rest with an average energy of $\langle E_\nu \rangle = 31.7$ MeV. Their reported result of the cross section is

$$\sigma(\nu_e e^-) = (3.18 \pm 0.56) \times 10^{-43} \text{cm}^2,$$

which is found to be consistent with the prediction of the standard model.

Table 9.3 Cross section of neutrino–electron $\nu_e e$ ($\bar{\nu}_e e$) scattering processes from different experiments. [a] Region in visible energy [1.5–3.0] MeV. [b] Region in visible energy [3.0–4.5] MeV.

Experiment	$\frac{\sigma(\nu_e e)}{E_{\nu_e}}(\times 10^{-42}\,\frac{cm^2}{GeV})$	$\sigma(\bar{\nu_e} e) \times 10^{-46} cm^2$	$\sin^2\theta_W$
Savannah River [354, 408]		7.6 ± 2.2^a	0.25 ± 0.05
(Reactor)		1.86 ± 0.48^b	
Kurchatov (Reactor) [409]		6.8 ± 4.5	0.29 ± 0.10
LAMPF E225 (LAMPF) [407]	$10.0 \pm 1.5 \pm 0.9$		0.249 ± 0.063
LSND [140]	$10.1 \pm 1.1 \pm 1.0$		

Moreover, $\nu_e e^-$ cross section measurements have been performed by the liquid scintillator neutrino detector (LSND) at the Los Alamos Neutron Science Center and 191±22 events were

https://doi.org/10.1017/9781108489065.010 Published online by Cambridge University Press

reported. The measured value of the cross section [140], given in Table 9.3, as well as the magnetic moment of the neutrino, given in Table 9.4, are consistent both with the E225 results

Table 9.4 Magnetic moment of neutrinos as measured by the different experiments [117].

Experiment	$\mu_{\nu_e}(\mu_B)$	$\mu_{\nu_\mu}(\mu_B)$
E225 (LAMPF)	$< 0.6 \times 10^{-9}$	
MUNU	$< 9.0 \times 10^{-11}$	
GEMMA	$< 2.9 \times 10^{-11}$	
TEXONO	$\leq 2.2 \times 10^{-10}$	
BOREXINO	$\leq 3.1 \times 10^{-11}$	
LSND	1.1×10^{-9}	6.8×10^{-10}
DONUT		3.9×10^{-7}
E734 (AGS)		$< 0.85 \times 10^{-9}$

as well as with the predictions of the standard model. Moreover, the cross section for the reaction $\bar{\nu}_e + e^- \rightarrow \bar{\nu}_e + e^-$ has also been determined with reactor antineutrinos at Savannah river and Kurchatov experiments.

9.5.1 Determination of the magnetic moment of neutrinos

In the standard model of electroweak interactions, neutrinos are massless and neutral. Therefore, these neutrinos can neither have a Dirac magnetic moment due to the absence of vector coupling of neutrinos with the photon field, nor can they have anomalous magnetic moment as it arises from chirality-flipping interactions and there are no right-chiral neutrinos in the standard model.

With the observation of neutrino oscillation phenomena, it is now well established that neutrinos have non-zero masses, while the absolute mass is yet to be determined for a particular flavor of neutrino. If the mass of the neutrino is taken into account, then one is discussing a physics beyond the standard model. In the minimal extension of the standard model, it is possible to include a finite neutrino mass and their interactions with the magnetic field. There are models which discuss the Dirac neutrinos with a finite magnetic dipole moment $\mu_\nu = \frac{3eG_F}{8\sqrt{2}\pi^2} m_{\nu_i} = 3.2 \times 10^{-19} \left(\frac{m_{\nu_i}}{eV}\right) \mu_B$ [117, 410].

In the standard model, $\nu_e(k) + e^-(p) \rightarrow \nu_e(k') + e^-(p')$ scattering takes place via the exchange of W^+ and Z^0 bosons and the corresponding diagrams are shown in Figure 9.10. However, if neutrinos have a magnetic moment, then there is an additional diagram which is possible through photon exchange as shown in Figure 9.11. The amplitude arising due to W^+ and Z^0 exchange, that is, $\mathcal{M}_W + \mathcal{M}_Z$ will not coherently add up to the amplitude arising from the photon exchange. This is because of the helicity of the outgoing neutrino which gets flipped due to magnetic moment coupling and will not be the same as obtained in the case of W^+ and Z^0 exchange.

https://doi.org/10.1017/9781108489065.010 Published online by Cambridge University Press

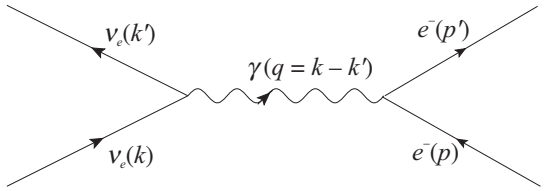

Figure 9.11 Neutral current reaction mediated by a photon.

The transition matrix element for the $\nu_e e^-$ scattering mediating through a γ-exchange is written as:

$$\mathcal{M}_\gamma = \mu_T \bar{u}(\vec{k}')i\sigma_{\mu\nu}q^\nu u(\vec{k})\frac{e}{q^2}\bar{u}(\vec{p}')\gamma^\mu u(\vec{p}), \tag{9.55}$$

where $\mu_T = \frac{e\mu_\nu}{2m_e}$ with μ_ν being the magnetic moment of the neutrinos.

Using the trace properties of the γ-matrices, the transition matrix element squared is obtained as:

$$|\mathcal{M}_\gamma|^2 = \frac{4\pi^2\alpha^2\mu_\nu^2}{m_e^2Q^2}\left[32\left\{k\cdot p'(2m_e^2 - p\cdot p') + k\cdot p(4k\cdot p' + p\cdot p' - 2m_e^2)\right\}\right]. \tag{9.56}$$

Using $|\mathcal{M}_\gamma|^2$ from Eq. (9.56), the differential scattering cross section in the Lab frame is obtained as:

$$\begin{aligned}\left.\frac{d\sigma}{d\Omega}\right|_\gamma &= \frac{\alpha^2\mu_\nu^2}{m_e^2E_\nu}\frac{E_e'}{m_e^2Q^2}\left\{E_e'(1-\cos\theta)(2m_e^2 - E_e'm_e) + m_e\left(4E_\nu E_e'(1-\cos\theta)\right.\right.\\ &+ \left.\left. E_e'm_e - 2m_e^2\right)\right\}.\end{aligned} \tag{9.57}$$

Therefore, the differential scattering cross section for the $\nu_e e^-$ scattering, where the magnetic moment of the neutrino has been taken into account, may be written as:

$$\left.\frac{d\sigma}{d\Omega}\right|_{\nu_e e^-} = \left.\frac{d\sigma}{d\Omega}\right|_{W+Z} + \left.\frac{d\sigma}{d\Omega}\right|_\gamma. \tag{9.58}$$

The expressions for $\left.\frac{d\sigma}{d\Omega}\right|_{W+Z}$ and $\left.\frac{d\sigma}{d\Omega}\right|_\gamma$ are given in Eqs. (9.52) and (9.57), respectively.

The upper limits on the magnetic moment of neutrinos have been determined by many experiments using neutrino–electron scattering. For example, MUNU, GEMMA, TEXONO, and DONUT experiments have determined an upper limit which are listed here in Table 9.4 [117].

9.6 $e^- + e^+ \longrightarrow \mu^- + \mu^+$

The process

$$e^-(E_e, \vec{k}) + e^+(E_e', \vec{k}') \longrightarrow \mu^-(E_\mu, \vec{p}) + \mu^+(E_\mu', \vec{p}') \tag{9.59}$$

https://doi.org/10.1017/9781108489065.010 Published online by Cambridge University Press

is induced by the exchange of a photon, a Z^0 boson as well as the Higgs boson in the standard model as shown in Figure 9.13. The quantities in the brackets are the four momenta of the incoming and outgoing particles, respectively. The Lagrangians for this process mediated by these bosons are, respectively, given by:

(i) photon exchange

$$L_\gamma = \sum_{l=e,\mu,\tau} \bar{\psi}_l(-\vec{p}\,')(-e\gamma^\mu)\psi_l(\vec{p})A_\mu. \tag{9.60}$$

(ii) Z^0 boson,

$$L_{Z^0} = \sum_{l=e,\mu,\tau} \bar{\psi}_l(-\vec{p}\,') \left(\frac{-g}{2\cos\theta_W}\right) \gamma^\mu(g_V^l - g_A^l\gamma^5)\psi_l(\vec{p})Z_\mu. \tag{9.61}$$

(iii) Higgs boson,

$$L_{\text{Higgs}} = \sum_{l=e,\mu,\tau} \bar{\psi}_l(-\vec{p}\,') \left(\frac{-m_l}{v}\right) \psi_l(\vec{p})\phi^*. \tag{9.62}$$

These interactions have also been represented by Feynman diagrams for photon, Z^0, and Higgs boson exchange, respectively as shown in Figure 9.12. Here, A^μ, Z^μ, and H^μ represent the photon, Z boson, and Higgs field, respectively and

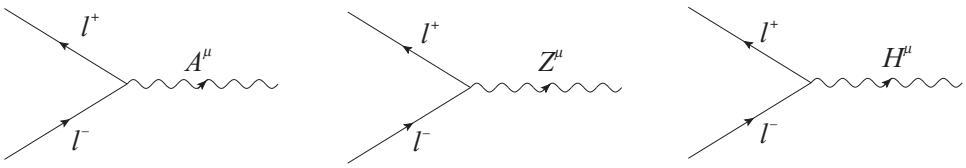

Figure 9.12 Interaction of charged leptons with photon, Z and Higgs fields.

$$\begin{aligned} g_V^l &= -\frac{1}{2} + 2\sin^2\theta_W, \\ g_A^l &= -\frac{1}{2}, \end{aligned}$$

where $l = e^-, \mu^-$. $\left(\frac{-m_l}{v}\right)$ represents the strength when leptons interact through Higgs boson, with

$$v = \frac{1}{\sqrt{\sqrt{2}G_F}} \approx 246\ \text{GeV}. \tag{9.63}$$

Using the Feynman rules, we can write the matrix element for the aforementioned diagrams. For a photon exchange, the matrix element is given as:

https://doi.org/10.1017/9781108489065.010 Published online by Cambridge University Press

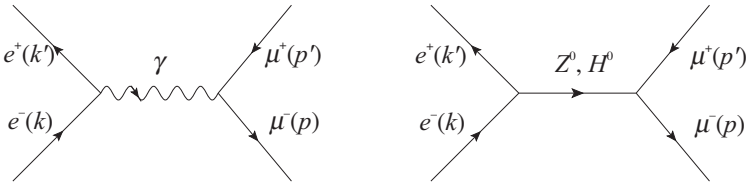

Figure 9.13 Feynman diagram for the $e^-e^+ \to \mu^-\mu^+$ via γ (left), Z^0, and H^0(right).

$$-i\mathcal{M}_\gamma = \left[ie\overline{v}(\vec{p}')\gamma_\mu u(\vec{p})\right]\left(\frac{-ig^{\mu\nu}}{q^2}\right)\left[ie\overline{v}(\vec{k}')\gamma_\nu u(\vec{k})\right],$$

where the four momentum transfer q is defined as $q = k + k'$.

$$\mathcal{M}_\gamma = -\frac{e^2}{q^2}\left[\overline{v}(\vec{p}')\gamma_\mu u(\vec{p})\right]\left[\overline{v}(\vec{k}')\gamma^\mu u(\vec{k})\right]. \tag{9.64}$$

For the Z^0 boson, the matrix element is given as:

$$\begin{aligned} -i\mathcal{M}_Z &= \left[\overline{v}(\vec{p}')i\left(\frac{-g}{2\cos\theta_W}\right)\gamma^\mu(g_V^l - g_A^l\gamma^5)u(\vec{p})\right]\left(-i\left(\frac{g_{\mu\nu} - \frac{q_\mu q_\nu}{M_Z^2}}{q^2 - M_Z^2}\right)\right) \\ &\times \left[\overline{v}(\vec{k}')i\left(\frac{-g}{2\cos\theta_W}\right)\gamma^\nu(g_V^l - g_A^l\gamma^5)u(\vec{k})\right]. \end{aligned}$$

In the limit $M_Z^2 >> q^2$, the transition matrix element is obtained as:

$$\mathcal{M}_Z = \sqrt{2}G_F\left[\overline{v}(\vec{p}')\gamma^\mu(g_V^l - g_A^l\gamma^5)u(\vec{p})\right]\left[\overline{v}(\vec{k}')\gamma_\mu(g_V^l - g_A^l\gamma^5)u(\vec{k})\right]. \tag{9.65}$$

For the Higgs boson, the matrix element is given as:

$$\mathcal{M}_H = \frac{m_e m_\mu}{v^2}\left[\overline{v}(\vec{p}')u(\vec{p})\right]\frac{1}{q^2 - M_H^2}\left[\overline{v}(\vec{k}')u(\vec{k})\right]. \tag{9.66}$$

The total Feynman amplitude is obtained by taking the contribution from all the three channels of the aforementioned process , that is, via γ, Z^0 and Higgs, that is,

$$\mathcal{M} = \mathcal{M}_\gamma + \mathcal{M}_Z + \mathcal{M}_H. \tag{9.67}$$

In order to obtain the differential and hence, the total scattering cross section, we have to calculate $|\mathcal{M}|^2$ which is obtained as:

$$\begin{aligned} \overline{\sum_i}\sum_f|\mathcal{M}|^2 &= \overline{\sum_i}\sum_f[(\mathcal{M}_\gamma + \mathcal{M}_Z + \mathcal{M}_H)^*(\mathcal{M}_\gamma + \mathcal{M}_Z + \mathcal{M}_H)] \\ &= \overline{\sum_i}\sum_f\Big[|\mathcal{M}_\gamma|^2 + |\mathcal{M}_Z|^2 + |\mathcal{M}_H|^2 + \mathcal{M}_\gamma^*\mathcal{M}_Z + \mathcal{M}_Z^*\mathcal{M}_\gamma \\ &+ \mathcal{M}_Z^*\mathcal{M}_H + \mathcal{M}_H^*\mathcal{M}_Z + \mathcal{M}_H^*\mathcal{M}_\gamma + \mathcal{M}_\gamma^*\mathcal{M}_H\Big], \end{aligned} \tag{9.68}$$

https://doi.org/10.1017/9781108489065.010 Published online by Cambridge University Press

where

$$\overline{\sum_i}\sum_f |\mathcal{M}_\gamma|^2 = \frac{e^4}{q^4}\left(8\left(m_e^2\left(2m_\mu^2 + p\cdot p'\right) + m_e^2 k\cdot k' + k\cdot p' k'\cdot p + k\cdot p k'\cdot p'\right)\right), \tag{9.69}$$

$$\begin{aligned}\overline{\sum_i}\sum_f |\mathcal{M}_Z|^2 = 2G_F^2\Big(8\Big(&2m_e^2 m_\mu^2 (g_A^{l^2} - g_V^{l^2})^2 - m_e^2(g_A^{l^4} - g_V^{l^4}) p\cdot p' \\ &- m_\mu^2 (g_A^{l^4} - g_V^{l^4}) k\cdot k' + k\cdot p' k'\cdot p\left(g_A^{l^4} + g_V^{l^4} - 2g_A^{l^2} g_V^{l^2}\right) \\ &+ k\cdot p k'\cdot p'\left(g_A^{l^4} + g_V^{l^4} + 6g_A^{l^2} g_V^{l^2}\right)\Big)\Big),\end{aligned} \tag{9.70}$$

$$\overline{\sum_i}\sum_f |\mathcal{M}_H|^2 = \frac{m_e^2 m_\mu^2}{v^4}\frac{1}{(q^2 - M_H^2)^2}\left(4\left({m_e}^2 - k\cdot k'\right)\left({m_\mu}^2 - p\cdot p'\right)\right), \tag{9.71}$$

$$\begin{aligned}\overline{\sum_i}\sum_f \mathcal{M}_\gamma^* \mathcal{M}_Z = \overline{\sum_i}\sum_f \mathcal{M}_\gamma \mathcal{M}_Z^* = \frac{e^2}{q^2}\sqrt{2}G_F\Big(8\Big(&2m_e^2 m_\mu^2 g_V^{l^2} + m_e^2 g_V^{l^2} p\cdot p' + m_\mu^2 g_V^{l^2} k\cdot k' \\ &+ k\cdot p' k'\cdot p(g_V^{l^2} - g_A^{l^2}) + k\cdot p k'\cdot p'(g_A^{l^2} + g_V^{l^2})\Big)\Big),\end{aligned} \tag{9.72}$$

$$\begin{aligned}\overline{\sum_i}\sum_f \mathcal{M}_\gamma^* \mathcal{M}_H = \overline{\sum_i}\sum_f \mathcal{M}_\gamma \mathcal{M}_H^* = \frac{e^2}{q^2}\frac{m_e m_\mu}{v^2}\frac{1}{q^2 - M_H^2}\big(&4m_e m_\mu (k\cdot p - k\cdot p' - k'\cdot p \\ &+ k'\cdot p')\big),\end{aligned} \tag{9.73}$$

$$\begin{aligned}\overline{\sum_i}\sum_f \mathcal{M}_H^* \mathcal{M}_Z = \overline{\sum_i}\sum_f \mathcal{M}_H \mathcal{M}_Z^* = \sqrt{2}G_F\frac{m_e m_\mu}{v^2}\frac{1}{q^2 - M_H^2}\Big(&4m_e m_\mu g_V^{l^2}(k\cdot p - k\cdot p' \\ &- k'\cdot p + k'\cdot p')\big).\end{aligned} \tag{9.74}$$

In the Lab frame, $\vec{k}' = 0$ and $\vec{p}\,' = \vec{k} + \vec{k}' = \vec{q}$, and the scalar products become

$$\begin{aligned} k\cdot k' &= m_e E_e,\ \ k'\cdot p = m_e E_\mu,\ \ k\cdot p = E_e E_\mu(1 - \cos\theta), \\ k\cdot p' &= m_e^2 + m_e E_e - E_e E_\mu(1 - \cos\theta), \\ p\cdot p' &= E_e E_\mu(1 - \cos\theta) + m_e E_\mu - m_\mu^2, \\ k'\cdot p' &= m_e E_e + m_e^2 - m_e E_\mu. \end{aligned}$$

The differential cross section in the Lab frame is evaluated in terms of the scalar products and is given as:

$$\begin{aligned}\left.\frac{d\sigma}{d\Omega}\right|_{\text{Lab}} = \frac{1}{32m_e^2\pi^2}\frac{E_\mu^2}{E_e^2}\Bigg(&-\frac{2m_e m_\mu^2 e^2\left(m_e^2 + m_\mu^2 - 2E_e E_\mu(1 - \cos\theta)\right)}{v^2(m_e + E_e)\left(2m_e^2 + 2m_e E_e - M_H^2\right)} \\ &- \frac{4\sqrt{2}m_e^2 m_\mu^2 G_F g_V^{l^2}\left(m_e^2 + m_\mu^2 - 2E_e E_\mu(1 - \cos\theta)\right)}{v^2\left(2m_e^2 + 2m_e E_e - M_H^2\right)}\end{aligned}$$

https://doi.org/10.1017/9781108489065.010 Published online by Cambridge University Press

$$
\begin{aligned}
&+ \frac{2m_e^2 m_\mu^2\left(-m_e^2+m_e(E_\mu-E_e)+m_\mu^2\right)\left(m_e^2-E_eE_\mu(1-\cos\theta)\right)}{v^4\left(-2m_e^2-2m_eE_e+M_H^2\right)^2}\\
&+ 8G_F^2\left(-m_e^3(g_A^{l4}-g_V^{l4})(m_e+E_e-E_\mu)+2m_e^2m_\mu^2(g_A^{l2}-g_V^{l2})^2\right.\\
&+ m_eE_\mu\left(g_A^{l2}-g_V^{l2}\right)^2\times\left(m_e^2+m_eE_e-E_eE_\mu(1-\cos\theta)\right)\\
&+ m_eE_e\left(g_A^{l4}+6g_A^{l2}g_V^{l2}+g_V^{l4}\right)\left(E_\mu(m_e+E_e(1-\cos\theta))\right.\\
&- \left.\left.m_\mu^2\right)+m_\mu^2E_eE_\mu(1-\cos\theta)\left(g_V^{l4}-g_A^{l4}\right)\right)+\frac{e^4}{m_e^2(m_e+E_e)^2}\left(m_e^4+m_e^3E_e\right.\\
&+ \left.2m_e^2\left(m_\mu^2+E_eE_\mu\right)-m_eE_e\left(m_\mu^2+E_\mu(E_\mu-E_e)(1-\cos\theta)\right)+m_\mu^2E_eE_\mu(1-\cos\theta)\right)\\
&+ \frac{1}{m_e(m_e+E_e)}4\sqrt{2}e^2G_F\left(m_e^4g_V^{l2}+m_e^3\left(E_eg_V^{l2}-E_\mu g_A^{l2}\right)+2m_e^2g_V^{l2}\left(m_\mu^2+E_eE_\mu\right)\right.\\
&+ m_eE_e\left(E_\mu\left(E_e(1-\cos\theta)\left(g_A^{l2}+g_V^{l2}\right)+E_\mu\left(g_A^{l2}-g_V^{l2}\right)\right)-m_\mu^2\left(g_A^{l2}+g_V^{l2}\right)\right)\\
&+ \left.\left.m_\mu^2E_eE_\mu(1-\cos\theta)g_V^{l2}\right)\right). \qquad (9.75)
\end{aligned}
$$

In the center of the mass frame, $\vec{k}=-\vec{k}'$, $E_e=E_e'=E_l$ and $E_\mu=E_\mu'=E_l$ and the scalar products become

$$
\begin{aligned}
k\cdot k' &= 2E_l^2-m_e^2,\\
k\cdot p &= E_l^2+\sqrt{(E_l^2-m_e^2)(E_l^2-m_\mu^2)}\cos\theta',\\
k\cdot p' &= E_l^2-\sqrt{(E_l^2-m_e^2)(E_l^2-m_\mu^2)}\cos\theta',\\
k'\cdot p &= E_l^2-\sqrt{(E_l^2-m_e^2)(E_l^2-m_\mu^2)}\cos\theta',\\
k'\cdot p' &= E_l^2+\sqrt{(E_l^2-m_e^2)(E_l^2-m_\mu^2)}\cos',\\
p\cdot p' &= 2E_l^2-m_e^2.
\end{aligned}
$$

Using these expressions, the differential scattering cross section in the center of mass frame is obtained as:

$$
\begin{aligned}
\left.\frac{d\sigma}{d\Omega}\right|_{CM} &= \frac{1}{128E_l^2\pi^2}\sqrt{\frac{m_\mu^2-E_l^2}{m_e^2-E_l^2}}\left[\frac{1}{E_l^2}4\sqrt{2}e^2G_F\left(g_V^{l2}\cos^2\theta'\left(m_e^2-E_l^2\right)\left(m_\mu^2-E_l^2\right)\right.\right.\\
&+ \left.\left.2E_l^2\cos\theta'g_A^{l2}\sqrt{\left(m_e^2-E_l^2\right)\left(m_\mu^2-E_l^2\right)}+E_l^2g_V^{l2}\left(m_e^2+m_\mu^2+E_l^2\right)\right)\right.\\
&+ \left.\frac{e^4}{2E_l^4}\left(\left(m_e^2\left(m_\mu^2\cos^2\theta'-\left(\cos^2\theta'-1\right)E_l^2\right)+E_l^2\left(\left(\cos^2\theta'+1\right)E_l^2\right.\right.\right.\right.
\end{aligned}
$$

https://doi.org/10.1017/9781108489065.010 Published online by Cambridge University Press

$$
\begin{aligned}
&- \quad m_\mu^2\left(\cos^2\theta'-1\right)\Big)\Big)\Big)+16G_F^2\Bigg(E_l^2\left(8\cos\theta' g_A^{l^2}g_V^{l^2}\sqrt{\left(m_e^2-E_l^2\right)\left(m_\mu^2-E_l^2\right)}\right.\\
&- \quad m_\mu^2\left(g_A^{l^2}+g_V^{l^2}\right)\left(\left(1+\cos^2\theta'\right)g_A^{l^2}\left(\cos^2\theta'-1\right)g_V^{l^2}\right)\\
&+ \quad \left(1+\cos^2\theta'\right)E_l^2\left(g_A^{l^2}+g_V^{l^2}\right)^2\Big)+m_e^2\left(m_\mu^2\left(\left(2+\cos^2\theta'\right)g_A^{l^4}\right.\right.\\
&+ \quad 2\left(\cos^2\theta'-1\right)g_A^{l^2}g_V^{l^2}+\cos^2\theta' g_V^{l^4}\Big)-E_l^2\left(g_A^{l^2}+g_V^{l^2}\right)\left(\left(\cos^2\theta'+1\right)g_A^{l^2}\right.\\
&+ \quad \left.\left.\left.\left(\cos^2\theta'-1\right)g_V^{l^2}\right)\right)\Big)+\frac{4m_e^2m_\mu^2e^2\cos\theta'\sqrt{\left(m_e^2-E_l^2\right)\left(m_\mu^2-E_l^2\right)}}{E_l^2v^2\left(4E_l^2-M_H^2\right)}\\
&+ \quad \frac{16\sqrt{2}m_e^2m_\mu^2\cos\theta' G_F g_V^{l^2}\sqrt{\left(m_e^2-E_l^2\right)\left(m_\mu^2-E_l^2\right)}}{v^2\left(4E_l^2-M_H^2\right)}\\
&+ \quad \left.\frac{8m_e^2m_\mu^2\left(m_e^2-E_l^2\right)\left(m_\mu^2-E_l^2\right)}{v^4\left(M_H^2-4E_l^2\right)^2}\right]. \qquad (9.76)
\end{aligned}
$$

Figure 9.14 presents the results for the angular distribution in the CM frame, that is, $\left.\frac{d\sigma}{d\Omega}\right|_{CM}$ for $e^-e^+ \longrightarrow \mu^-\mu^+$ scattering process at various CM energies.

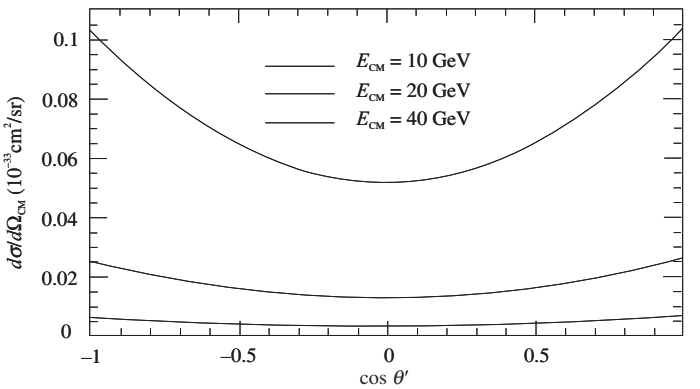

Figure 9.14 $d\sigma/d\Omega|_{CM}$ vs. $\cos\theta'$ at different values of center of mass energies, viz., $E_{CM} = 10$, 20, and 40 GeV for the process $e^- + e^+ \longrightarrow \mu^- + \mu^+$.

In Figure 9.15, the results for the contribution to the cross section from each term, that is, photon exchange, Z^0 exchange, and Higgs exchange for the CM energy of 10, 30, 50, and 90 GeV are presented. At low CM energies ($E_{CM} = \sqrt{s} \leq 10$ GeV), the effect of Z^0 is almost negligible and with the increase in CM energy, the contribution of Z^0 increases. It may be observed that for the CM energy close to the mass of Z^0 boson (i.e., at Z^0 pole), the cross section for $e^-e^+ \longrightarrow \mu^-\mu^+$ mediated by Z^0 becomes large.

https://doi.org/10.1017/9781108489065.010 Published online by Cambridge University Press

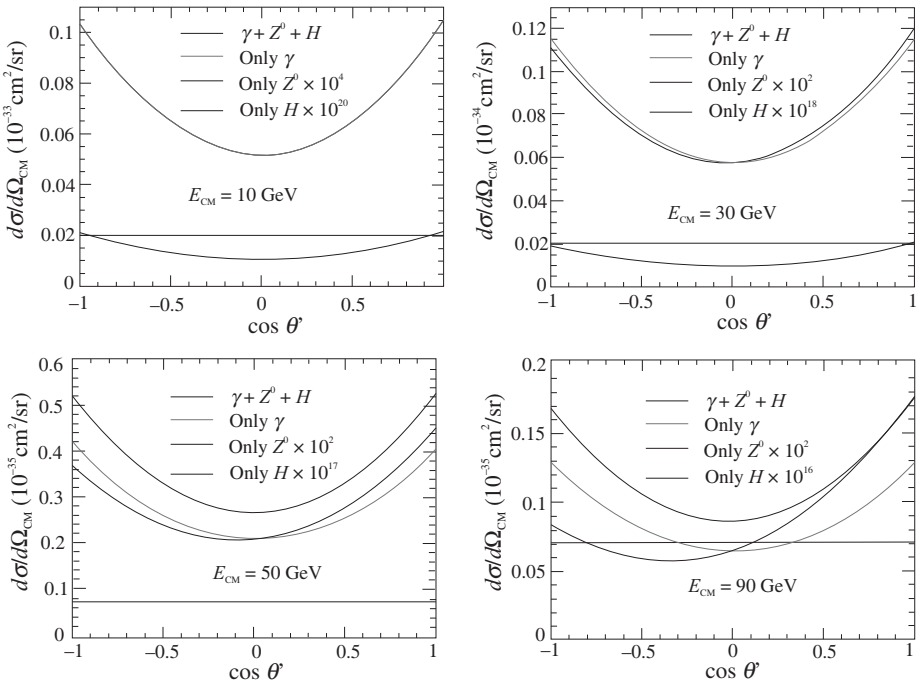

Figure 9.15 Comparison of the differential cross section with different propagators at $E_{CM} = 10$ GeV (upper left panel), 30 GeV (upper right panel), 50 GeV (lower left panel), and 90 GeV (lower right panel) for the process $e^- + e^+ \longrightarrow \mu^- + \mu^+$.

e^-e^+ collision experiments have been performed to measure energy or angular distribution for $e^-e^+ \rightarrow l^-l^+$ like at PEP, PETRA, TRISTAN, LEP, etc. laboratories. For example, at PETRA [411], measurements of the angular distributions have been performed in the different energy ranges ($\sqrt{s} = 13, 17, 27.4, 30,$ and 31.6 GeV) for $e^-e^+ \longrightarrow l^-l^+$ ($l = e, \mu, \tau$). Using these experimental data, Marshall et al. (1985) [412] extracted the values of $g_V^e g_V^\mu$, $g_V^e g_V^\tau$, $g_A^e g_A^\mu$, $g_A^e g_A^\tau$. These results are consistent with the standard model prediction with $\sin^2\theta_W = 0.23$. Moreover, an analysis was performed to obtain the squares of the couplings assuming $e - \mu - \tau$ universality. It was found that $\left(g_V^e\right)^2 = 0.012 \pm 0.029$ and $\left(g_A^e\right)^2 = 0.268 \pm 0.024$. Using these results and the results from $\nu_e e^-$ scattering experiments, it was concluded that $g_V^e \sim 0$ and $g_A^e \sim -0.5$ are the most acceptable results [413] that are comparable with the value of $g_V^e = -\frac{1}{2} + 2\sin^2\theta_W$ and $g_A^e = -\frac{1}{2}$ predicted by the standard model.

https://doi.org/10.1017/9781108489065.010 Published online by Cambridge University Press